DyeIonogels: Proton-Responsive Ionogels Based on a Dye-Ionic Liquid Exhibiting Reversible Color Change

Zai-Lai Xie, Xing Huang, and Andreas Taubert**

Transparent, ion-conducting, and flexible ionogels based on the room temperature ionic liquid (IL) 1-butyl-3-methylimidazolium bis(trifluoromethane sulfonyl)imide [Bmim][N(Tf)$_2$], the dye-IL (DIL) 1-butyl-3-methylimidazolium methyl orange [Bmim][MO], and poly(methylmethacrylate) (PMMA) are prepared. Upon IL incorporation the thermal stability of the PMMA matrix significantly increases from 220 to 280 °C. The ionogels have a relatively high ionic conductivity of 10^{-4} S cm^{-1} at 373 K. Most importantly, the ionogels exhibit a strong and reversible color change when exposed to aqueous or organic solutions containing protons or hydroxide ions. The resulting material is thus a prototype of soft multifunctional matter featuring ionic conductivity, easy processability, response to changes in the environment, and a strong readout signal, the color change, that could be used in optical data storage or environmental sensing.

1. Introduction

Ionic liquids (ILs) have attracted continuous interest because of their remarkable physico-chemical properties, including high thermal and chemical stability, non-flammability, negligible vapor pressure, electrical and ionic conductivity, low melting point, and affinity for many compounds.[1–5] The key advantage of ILs over molecular liquids is that by smart selection of the IL anion and cation, the properties of ILs can be tuned to satisfy specific requirements, where molecular compounds are often not suitable or at least inefficient.[6–8] As a result, materials science has embraced ILs for the synthesis of new materials but also as functional components in advanced multifunctional hybrid materials such as ionogels.[9–15]

Ionogels are functional hybrid materials, which enable the development of devices combining the properties of the IL (e.g., ionic conductivity or thermal stability) and those of a host (e.g., transparency or mechanical stability).[12,13,16,17] Recent results demonstrate that ionogels often retain the dynamic features of the IL in the liquid state[15,18–20] and also influence the properties of the solid matrix material.[14] This endows ionogels with adjustable properties suitable for numerous applications including catalysis,[21,22] optical[23,24] and magnetic devices,[25] or fuel cells.[26–28] In all cases, the properties of the hybrid material (the ionogel) are directly related to the properties of the IL.[29,30]

As of now, most ionogels have been derived from commercial ILs and the corresponding studies essentially focus on the fundamental characteristics such as phase behavior, mechanical behavior, or ionic conductivity of the respective ionogels. In contrast, there are only few examples where the IL used for ionogels fabrication carries additional functionalities such as magnetism, luminescence, or responsiveness to stimuli such as temperature or pH. Xie et al. have used [Bmim][$FeCl_4$] and PMMA for the assembly of a weakly magnetic ionogel.[25] Binnemans et al. and Xie et al. have reported luminescent ionogels with enhanced lifetimes.[23,24] Benito-Lopez et al. have developed photoresponsive ionogels based on (poly(N-isopropylacrylamide) (pNIPAAM)), a photo-responsive spiropyran (SP), and phosphonium ILs for fluid control in microfluidics.[31] The same authors have also incorporated dyes such as bromophenyl blue, bromophenyl green, and bromophenyl purple into polymers to prepare ionogels responding to changes in the composition of aqueous solutions.[32] Although still sparse, these few examples illustrate that the addition of functional components in principle enables the fabrication of a large number of functional ionogels.[12,33–35]

One issue to overcome is the limited solubility of many active components such as dye molecules in ILs. There is thus a need to develop highly soluble active components, but so far, there are only a few examples.[36,37] In this contribution, we therefore describe a new approach towards responsive ionogels exhibiting a reversible color change. The ionogels are based on the dye-IL (DIL) 1-butyl-3-methylimidazolium methyl orange [Bmim][MO]. The combination of [Bmim][MO] with a PMMA matrix and with the IL 1-butyl-3-methylimidazolium bis(trifluoromethane sulfonyl)imide [Bmim][N(Tf)$_2$] yields transparent, flexible, ion conducting ionogels that reversibly respond to changes in proton concentration suggesting application as soft chemical sensor or in optical data storage.

2. Results

Orange solid [Bmim][MO] forms via anion exchange of sodium methyl orange at room temperature. Scanning electron

Dr. Z.-L. Xie, Prof. A. Taubert
Institute of Chemistry
University of Potsdam
D-14476, Potsdam, Germany
E-mail: xzlai@fhi-berlin.mpg.de;
ataubert@uni-potsdam.de
Dr. Z.-L. Xie, Dr. X. Huang
Fritz-Haber Institute of Max Planck Society
D-14195, Berlin, Germany

DOI: 10.1002/adfm.201303016

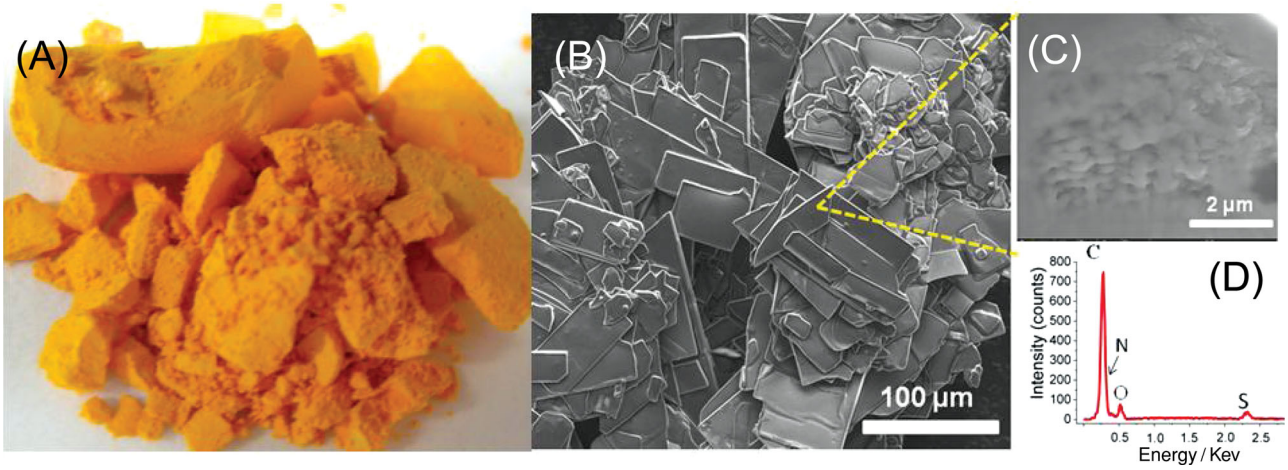

Figure 1. A) Photograph, B,C) SEM images, and D) EDX spectrum of [Bmim][MO].

microscopy (SEM) images clearly show that the samples of [Bmim][MO] are homogenous and contain particles with lath-like shapes in the micrometer size range. High magnification images show a sub-structure of interconnected, roughly spherical, particles suggesting that the lath-like particles could in fact be mesocrystals (**Figure 1**).[38] Indeed, selected-area electron diffraction and X-ray diffraction (XRD) support the formation of crystalline materials (Figure S1, Supporting Information). Energy dispersive X-ray spectroscopy (EDXS) indicates no sodium and chloride impurities from raw materials in the final [Bmim][MO].

Figure 2 shows photographs of PMMA ionogels prepared with [Bmim][MO] alone and with [Bmim][MO] dissolved in [Bmim][$N(Tf)_2$], respectively. Owing to the high melting point of [Bmim][MO] of 180 °C the ionogel prepared with [Bmim][MO] alone is turbid, indicating the formation of crystalline [Bmim][MO] within the PMMA matrix. In contrast, the samples prepared with [Bmim][MO] dissolved in [Bmim][$N(Tf)_2$]—denoted [Bmim][MO]@[Bmim][$N(Tf)_2$] from here on—is yellow and transparent, indicating the formation of a true ionogel. Moreover, the uniform color of both material types indicates that all materials are homogeneous, consistent with previous reports on similar systems.[23]

SEM images of the ionogels are shown in Figures 2C,D. No obvious phase separation is observed in the ionogel prepared with [Bmim][MO]@[Bmim][$N(Tf)_2$]; the only features are due to solvent evaporation during film casting. This suggests that [Bmim][MO] is dispersed homogeneously in the [Bmim][$N(Tf)_2$] and the PMMA matrix and does not crystallize. In contrast, the worm-like structure shown in Figure 2D is representative

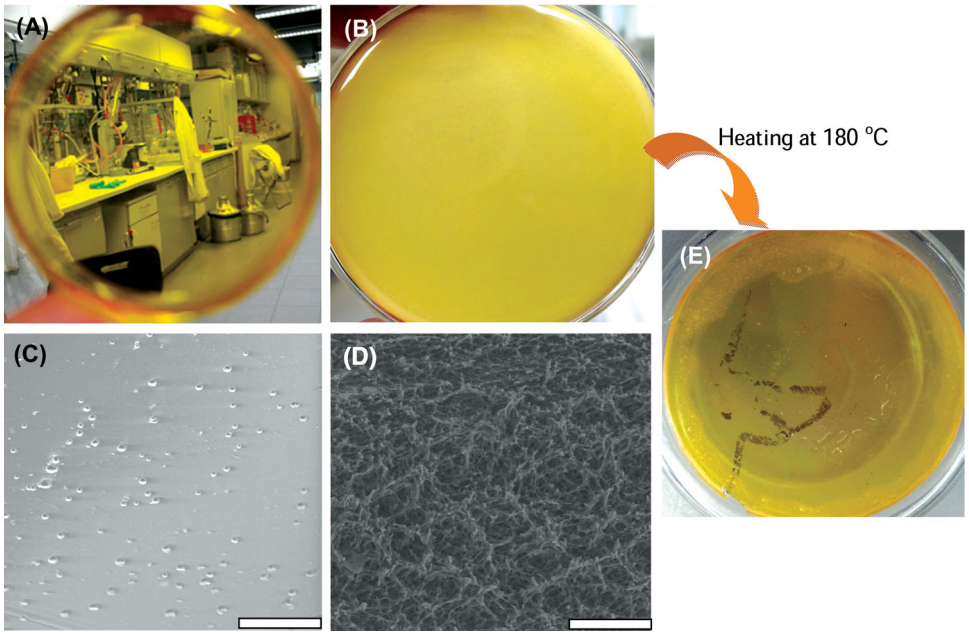

Figure 2. Photographs and SEM images of ionogels. A,C) Ionogel from [Bmim][MO]@[Bmim][$N(Tf)_2$] and PMMA. B,D) Ionogel from [Bmim][MO] alone in PMMA. E) [Bmim][MO] ionogels become transparent at 180 °C. Scale bars are 20 µm.

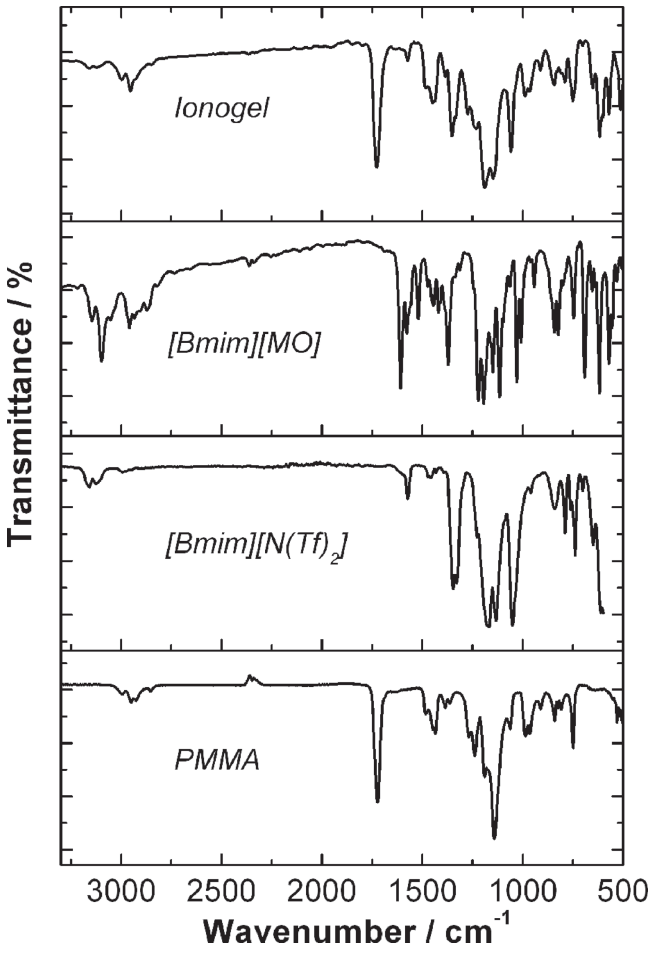

Figure 3. IR spectra of pure [Bmim][$N(Tf)_2$], pure [Bmim][MO], pure PMMA, and an ionogel with ≈30% of [Bmim][MO]@[Bmim][$N(Tf)_2$].

of ionogels prepared with [Bmim][MO] alone. This confirms our previous assumption that [Bmim][MO] alone crystallizes in the PMMA matrix and is thus responsible for the turbidity observed in ionogels prepared from [Bmim][MO] alone. SEM images of pure PMMA films could not be obtained since the electron beam induces very rapid degradation of the PMMA. Addition of the ILs significantly improves this.

Figure 3 shows IR spectra of pure [Bmim][MO], pure [Bmim][$N(Tf)_2$], pure PMMA, and an ionogel with ≈30 wt% of [Bmim][MO]@[Bmim][$N(Tf)_2$]. In the IR spectra of [Bmim][$N(Tf)_2$], the bands at 3162 and 3123 cm^{-1} are assigned to the C–H vibration of cyclic $[Bmim]^+$, whereas the bands at 2990, 1430, 829, and 736 cm^{-1} are assigned to aliphatic C–H vibrations from the $[Bmim]^+$ cation. The band at 1566 cm^{-1} stems from C–C and C–N bending vibrations in [Bmim][$N(Tf)_2$]. The signal at 1344 cm^{-1} is assigned to the asymmetric stretching mode of $–SO_2–$ in $[N(Tf)_2]^-$. In contrast to [Bmim][$N(Tf)_2$], a characteristic band at 1609 cm^{-1} is observed in the IR spectrum of [Bmim][MO], which is the vibration of the –N=N– group. Spectra of pure PMMA show a strong band at 1724 cm^{-1} from the PMMA carbonyl group. The bands at 1270, 1140, and 983 cm^{-1} are assigned to C–O–C stretching vibrations of PMMA (**Table 1**). The fact that the IR spectra of the ionogels essentially are a superposition of the spectra of the individual components is an indication that the materials are homogeneous but that there presumably is only little interaction between, for example, the PMMA and the IL.

Thermogravimetric analysis (TGA) shows that the main PMMA decomposition begins at 220 °C, leaving essentially no residue at ≈400 °C (**Figure 4**). This main weight loss is preceded by a loss of ≈2% assigned to the removal of residual water, possibly traces of acetone from the preparation process. Consistent with literature[23] [Bmim][$N(Tf)_2$] decomposes in one step with an onset at ca. 300 °C in dynamic TGA. In contrast to PMMA and [Bmim][$N(Tf)_2$], the ionogel shows two separate weight losses. The first weight loss occurs at higher temperatures than the decomposition of pure PMMA (280 instead of

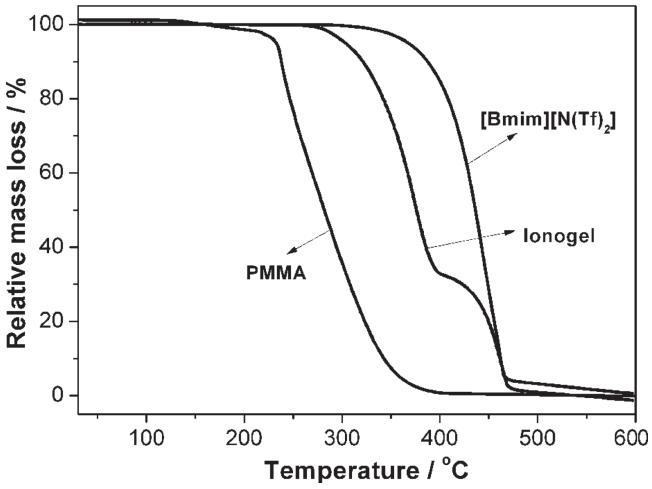

Figure 4. TGA curves of PMMA and ionogel with 30 wt% IL. Heating rate is 10 °C min^{-1} in air.

Table 1. Position and assignment of important IR signals.

Materials	IR (cm^{-1})					$\nu(–SO_2)$	$\nu(–N=N–)$
	ν (C=O)	ν (C–C/N from $[Bmim]^+$)	ν (C–H from aromatic)	ν (C–H_2)	ν (C–O–C)		
PMMA	1723	no	no	2950, 2925, 1434, 1238, 958, 838, 746	1270, 1140, 983	no	no
[Bmim][$N(Tf)_2$]	no	1569	3162, 3123, 1160, 636, 612	2990, 1430, 958, 829, 739	no	1344, 1049	no
[Bmim][MO]	no	1569	3152, 3099, 1160, 636, 612	2960, 2870,1434, 958, 841, 746	no	1359	1609
Ionogel	1728	1569	3158, 3110, 1160, 636, 612	2962, 2931, 2872, 1459, 1151, 828, 736	1272, 1150, 984	1346	no

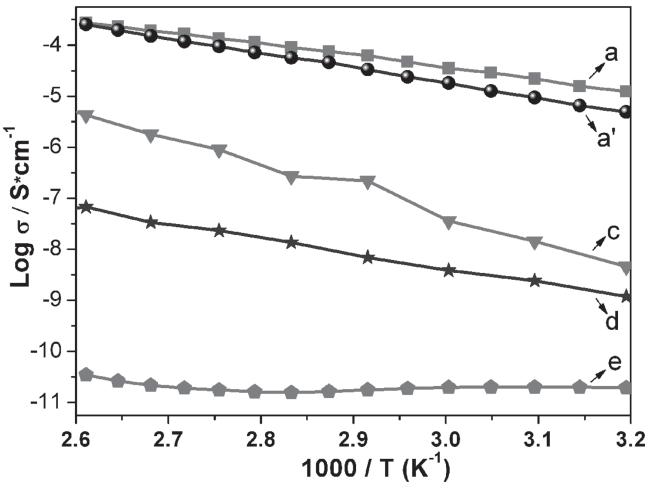

Figure 5. Temperature-dependent ionic conductivities. a and a' are the data for ionogels with 30 wt% [Bmim][N(Tf)$_2$] before and after exposure to aqueous HCl solution (see below); c and d are data of ionogels with 10 and 5 wt% of [Bmim][N(Tf)$_2$]; e is the dataset for pure PMMA.

220 °C). The onset of the second weight loss is ≈390 °C, which is again higher than the onset observed for the pure IL at ≈300 °C. The relative intensity of the two weight losses is proportional to the weight fraction of PMMA and IL in the ionogel. TGA thus shows that the IL, similar to earlier work,[19,20,35,39] significantly increases the thermal stability of PMMA ionogels in dynamic TGA.

Figure 5 shows the temperature-dependent ionic conductivities (σ) of an ionogel with 30 wt% [Bmim][N(Tf)$_2$] and pure PMMA between 0 and 100 °C. σ of the ionogel is 10^{-4} S cm^{-1} at 373 K (100 °C) and approximately seven orders of magnitude higher than σ of pure PMMA. σ decreases with decreasing IL content. The Arrhenius plots of the temperature dependency of σ of the ionogel can be fitted with the Vogel-Tamman-Fulcher (VTF) equation for the conductivity of electrolytic materials. The VTF equation is $\sigma = \sigma_0 \exp[-B/(T - T_0)]$, where the constants, σ_0 (S cm^{-1}), B (K), and T_0 (K) are adjustable parameters. The fitting parameter (R) of the ionogels is higher than 0.999.

Figure 6 shows the response of the ionogels towards acidic liquids. Two systems were investigated: i) a solution containing trifluoroacetic acid in hexane and ii) HCl in water. The acid concentrations ranged from 10^{-4} to 10^{-1} M and also included an acid-free control experiment, where the ionogels were exposed to the pure solvents. Figure 6 shows that all ionogels change their color on exposure to acids; this is due to the presence of the [Bmim][MO] within the ionogels. The color change is fast and occurs within a few seconds. Moreover, the color change is not abrupt but rather gradual, allowing the quantification or at least estimation of proton concentrations in a solvent. The reaction is reversible and upon addition of a base, the ionogels revert to their original yellow color, again after only a few seconds.

Figure 7 shows the corresponding reflectance UV/Vis spectra. Reflectance spectroscopy shows that the ionogels behave differently in water/HCl and hexane/trifluoroacetic acid mixtures in terms of the proton sensitivity: in hexane, the color change occurs already at fairly low proton concentrations; samples exposed to solutions with proton concentrations of 10^{-4} and 10^{-3} mol L^{-1} already show a significant shift of the absorption edge from 480 to 550 nm and then further to 580 nm at 10^{-2} mol L^{-1} and finally 608 nm at 10^{-1} mol L^{-1}. In contrast, the reflectance edge of the as-synthesized ionogels is roughly 480 nm. In aqueous solution, the sensitivity is lower and a no significant shift is observed until acid concentrations of 10^{-2} mol L^{-1}. The absorption edge shifts to 530, 550, and 560 nm for 10^{-2}, 10^{-1}, and 1 M solutions, respectively. This is again consistent with the color change shown in Figure 6.

To evaluate the stability of the ionogels against leaching, several leaching experiments were performed using UV-VIS spectroscopy for quantification (Figure S2, Supporting Information). In the case of aqueous HCl solutions ([H$^+$] = 0.1 M) a steady state is reached after ≈20 min. Moreover, the gels remain intact even after soaking for 20 hours. The highest leakage observed is 1.7% of the total amount of [Bmim][MO].

In the case of hexane/trifluoroacetic acid solutions ([H$^+$] = 0.05 M) an even lower leakage of at most 0.4 wt% of the total [Bmim][MO] content is observed. The lower leaching into hexane (compared to water) may be due to the lower solubility of [Bmim][MO] in hexane. Moreover, in contrast to the ionogels exposed to aqueous solutions, ionogels exposed to hexane/trifluoroacetic acid become soft and sticky after soaking for over 5 min. We currently assign this to a degradation of the PMMA by the trifluoroacetic acid. Note, however, that the color change of the ionogels happens in a few seconds. This suggests that the stability of the ionogels will, even in organic solvents, be sufficient for some applications. Clearly, the current ionogels

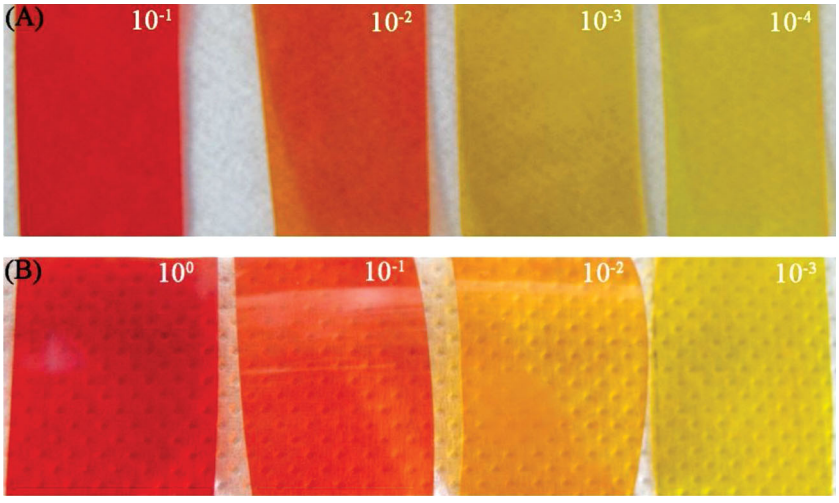

Figure 6. Color changes of ionogels exposed to A) aqueous HCl and B) hexane/trifluoroacetic acid. Numbers are concentrations of respective acid (mol L^{-1}).

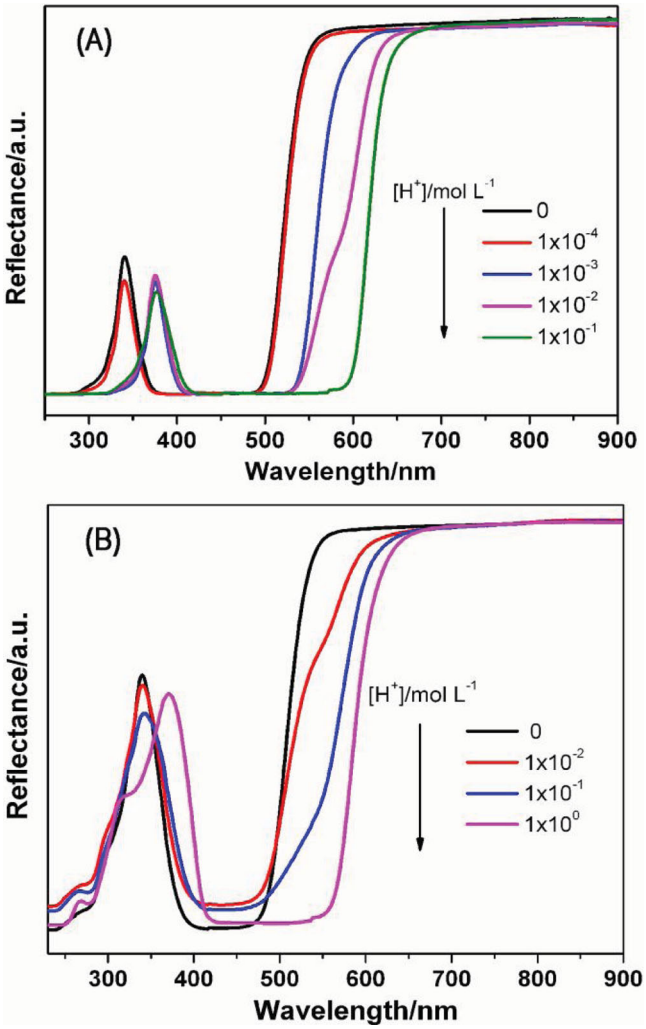

Figure 7. UV-Vis spectra of ionogels after soaking in A) water/HCl and B) hexane/trifluoroacetic acid solutions.

are not suitable for long-term proton monitoring in organic solvents, but rather for aqueous media.

As the dye is protonated (and thus charged) in acidic environments, the most prominent leaching is observed into acidic media. Further experiments with increasing volumes of aqueous HCl (Figure S3, Supporting Information) have however shown that increasing volumes of soaking solution do not lead to a more pronounced leaking of dye or IL. Instead, the apparent amount of leached DIL decreases with increasing volume of soaking solution. Clearly, this is due to a dilution effect. Recalculation of the amounts of leached DIL for 1 mL of soaking solution indeed shows that in all cases the amount of DIL in the soaking solution is between 1.4 and 1.9 ppm, regardless of the volume of the initial soaking solution. This thus shows that larger liquid volumes will not lead to a stronger leaching of dye or IL from the ionogel and suggests that even extended soaking (at least in aqueous media) will not lead to further leaching. This will however have to be studied in detail in the future.

3. Discussion

Functional ILs have received much attention as device components in chemical sensors, fuel cells, and batteries.[5,11,40,41] For IL-based devices, constructing solid state platforms with ionic liquid-like (multi)functionality is of exceptional technological importance because the confinement or trapping of an IL in the solid state of an ionogel eliminates many drawbacks associated with the liquid state such as leaking into other device components and issues with electrical connectors. The immobilization of ILs within polymers is therefore a highly promising approach towards a wide variety of new functional materials.

The current study focuses on soft, flexible, and proton-responsive ionogels by integrating the dye-IL (DIL) [Bmim][MO] into [Bmim][$N(Tf)_2$]/PMMA ionogels. The rationale for using mixtures of [Bmim][MO] and [Bmim][$N(Tf)_2$] rather than pure [Bmim][MO] is the high melting point and correspondingly high viscosity of [Bmim][MO]. Moreover, optical inspection of ionogels prepared with pure [Bmim][MO] (Figure 1) suggests that the IL does crystallize within the PMMA matrix at low temperatures yielding opaque films (Figure 2), which may—depending on the application—be undesirable.

Optical inspection and SEM of the ionogels (Figure 2), IR spectroscopy (Figure 3), and TGA (Figure 4) suggest that the materials are homogeneous and have no significant defects. The fact that there is virtually no shift in the IR bands as the IL is incorporated into the PMMA suggests that the interaction between the IL and PMMA is rather weak.[25] Although polymer-based ionogels have been studied in the recent past, the exact nature of the IL-polymer matrix interaction is still not fully resolved. Lodge et al. have shown that polymeric networks act like a sponge, where the holes are entirely filled with IL.[12,34] Watanabe and co-workers concluded that there are specific interactions between PMMA and the IL anion, which hamper the formation of ion clusters and associates.[19] Xie et al. have shown that 1-butyl-3-methylimidazolium tetrachloridoferrate(III), [Bmim][$FeCl_4$], is homogeneously distributed in PMMA even at high IL weight fractions, suggesting that there is a large miscibility window of the two components.[25] In the current case, optical inspection, IR spectroscopy, and TGA show that the ionogels are homogeneous, suggesting that various interactions with the ester groups or the hydrophobic parts of the PMMA with the IL are crucial for yielding a homogeneous material, similar to previous examples.[23,25]

In spite of the open questions with respect to the exact interaction and structure of ILs in (polymer) ionogels, the current study confirms previous data where ILs have been shown to increase the thermal stability of ionogels. Watanabe et al. have reported a higher thermal stability for PMMA after combination with [Bmim][$N(Tf)_2$] than for bulk PMMA.[19] The thermal stability of the ionogels increases from 257 °C to 285 °C despite the decreasing T_g with increasing [Bmim][$N(Tf)_2$] content.[23] A similar behavior has also been observed in the ionogels studied here (TGA, Figure 4). The onset of the weight loss is 220 °C for bulk PMMA and close to 280 °C for PMMA/[Bmim][$N(Tf)_2$] with 30% of IL.

The ionic conductivity of the current ionogels is around 10^{-4} S cm^{-1} at 100 °C (Figure 5), similar to other examples.[17]

Watanabe et al. have reported σ values of almost 10^{-5} S cm^{-1} with low [Emim][N(Tf)$_2$] at 30 °C.[19] This behavior has been assigned to the high self-dissociating and ion-transporting ability of the IL and the decoupling of the ion transport from polymer segmental motion.

The key novelty of the ionogels presented here is that they are sensitive to protons in both aqueous and non-aqueous solutions, although with different sensitivities.

The reason for the lower sensitivity in the aqueous system is probably the lower proton transfer rates from the aqueous phase to the hydrophobic IL. Notably, the ionogels remain flexible and transparent throughout the color change process, suggesting an application in the long term monitoring of, for example pH changes in (aqueous) solution or gas concentrations such as HCl or NH_3 in air. This concept is based on one key advantage of ILs and ionogels, the fact that the IL does not evaporate and, as it is hygroscopic, will always contain a few percent of water (unless used in high vacuum). This enables proton transport within the ionogel (and thus the response to incoming acidic and basic molecules). As a result, gas phase monitoring could be an interesting field of application for our dye-modified ionogels. In terms of the mechanism of proton response of the [Bmim][MO], we presume that it is identical to the color change in aqueous solution (Scheme S1, Supporting Information),[42] but this will have to be verified in the future, for example via NMR spectroscopy.

It is worthy to mention that we have also attempted to incorporate commercial methyl orange (which comes as a sodium salt) into the ionogels. However, these attempts failed owing to the poor solubility of methyl orange in most non-aqueous systems, including ILs. In contrast, [Bmim][MO] is soluble in [Bmim][N(Tf)$_2$] enabling the fabrication of dye-modified ionogels such as the ones presented here. DILs such as [Bmim][MO] therefore enable the fabrication of new (multi)functional soft matter based on components that are easily available. This strategy can be expanded to other IL-modified dyes or fluorescence dyes providing access to a multitude of responsive ILs, ionic liquid crystals, and ionogels. One possibility to improve the stability of the current materials against leaching (Figures S2, S3) could also include the use of more lipophilic dyes or more lipophilic imidazolium derivatives; these studies are currently underway.

Another feature to explore in the future is DILs with a lower melting point or liquid crystalline DILs. Such materials could combine the color change illustrated in the current study with a second, for example clear-opaque or even a clear-birefringent-opaque, transition. As the color change is proton-induced and the optical transparency is temperature-induced (Figure 2E), the current ionogel is a first prototype of a material that independently responds to external two triggers, protons and temperature.

4. Conclusion

The current study describes a new soft (multi)functional material, ionogels containing a dye-based IL as the active component. The ionogels are prototypes of a conductive and soft material showing reversible response to environmental conditions, specifically protons. The ionogels could thus find application in (gas or aqueous phase) sensing or serve as prototypes for responsive soft materials where protons and hydroxide ions could be used to deliberately induce color changes, for example in optical data storage technologies.

5. Experimental Section

Materials: Methyl methacrylate (MMA, Aldrich, 99%) was distilled under high vacuum before use to remove the inhibitor. 1-butyl-3-methylimidazolium chloride [Bmim][Cl] and 1-butyl-3-methylimidazolium bis(trifluoromethane sulfonyl)imide [Bmim][N(Tf)$_2$] (IoLiTec), methyl orange (Sigma, 98%), trifluoroacetic acid (Sigma, 99%), dichloromethane, methanol, and acetone (Merck) were used as received.

[Bmim][MO] Synthesis: 1 g of [Bmim]Cl was dissolved in 50 mL of acetone. Then sodium methyl orange (1.1 equiv) was added. The mixture was stirred at room temperature for 3 days. Sodium chloride salts were removed from the mixture by filtration. The filtrate was collected and the solvent was evaporated under vacuum. The orange [Bmim][MO] was obtained with the yield of 85%. Elemental analysis: calc. C 59.97%, H 6.59%, N 15.79%, S 7.23%. Found: C 59.90%, H 6.68%, N 15.81%, S 7.29%. ^{1}H NMR (300 MHz, $(CD_3)_2CO$): δ = 9.978 (1H, s), 7.928–7.768 (8H, m), 6.893–6.839 (2H, q), 4.454–4.373 (2H, t), 4.028 (3H, s), 3.111 (6H, s), 1.927–1.897 (2H, m), 1.452–1.401 (2H, m) 0.968–0.919 (3H, t).

Poly(methyl methacrylate): PMMA was synthesized by bulk free radical polymerization. MMA was purged with N_2 for about 20 min. to remove oxygen. 1 wt% of AIBN was dissolved in MMA under nitrogen. The polymerization was conducted at 60 °C for 30 min. and stopped before gelation by precipitating the polymer from methanol. Further purification was done by dissolution in acetone and precipitation in methanol, followed by drying under high vacuum. GPC: M_n = 118'100 g mol^{-1}. Molecular weight distributions were obtained by SEC using an Agilent 1200 isocratic pump, an Agilent 1200 refractive index detector, and three SDV columns (8 mm × 300 mm, particle size 5 µm, pore sizes 100, 1000, and 100 000 Å) from PSS. Elemental analysis: calc. C 59.96%, H 8.06%. Found: C 59.76%, H 8.12%.

Ionogels: Ionogels were prepared by mixing [Bmim][N(Tf)$_2$] (0.215 g) and [Bmim][MO] (0.002 g) with a solution of PMMA (0.500 g) in 10 mL of acetone. The yellow, transparent, and viscous mixture was cast in Petri dishes and allowed to dry for 24 h at room temperature followed by drying under vacuum for several days.

Thermal Analysis: Thermogravimetric analysis (TGA) was done in air on a Linseis L 81 thermal balance in air from 20 to 900 °C at 10 K min^{-1}.

Ionic Conductivity Measurements: Ionic conductivities were determined using the complex impedance method by varying the temperature from 293 to 252 K, then from 252 to 343 K, and finally from 343 to 293 K. The alternating-current (ac) conductivity measurements were carried out on a Solartron 1170 frequency response analyzer from 10 Hz to 1 MHz. The perturbation amplitude was 1.5 V. Ten points per decade were measured. The conductivity (σ) was determined from Arrhenius plots (log (σt) vs 1000/T).

Spectroscopy: IR spectra were recorded in attenuated total reflection (ATR) mode on a Thermo Nicolet FT-IR Nexus 470. UV/Vis spectra were recorded on an Agilent 8453 or a Perkin-Elmer Lambda 25 UV-Vis spectrometer at room temperature. Solution NMR spectra were measured on a Bruker Avance 300 with tetramethylsilane as internal standard.

Electron Microscopy: The morphologies of the samples were characterized using a Hitachi S4800 scanning electron microscope (SEM) operated at 2.0 kV. TEM and selected-area electron diffraction were recorded on a JEM-2100F operated at 200 kV.

Supporting Information

Supporting Information is available from the Wiley Online Library or from the author.

Acknowledgements

The authors thank Dr. F.-P. Wang for help with conductivity measurements and Dr. W. Qi for TGA mesurements. The Max Planck Institute of Colloids and Interfaces (Colloid Chemistry Department) and the University of Potsdam are acknowledged for financial support. Z.-L.X. acknowledges a Chinese Science Council Doctoral Fellowship.

Received: August 29, 2013
Revised: November 8, 2013
Published online: January 23, 2014

[1] P. Wasserscheid, T. Welton, *Ionic Liquids in Synthesis* Wiley-VCH, Weinheim **2008**.
[2] R. D. Rogers, K. R. Seddon, *Science* **2003**, *302*, 792–793.
[3] A. Taubert, *Topics Curr. Chem.* **2009**, *290*, 127.
[4] T. Ueki, M. Watanabe, *Macromolecules* **2008**, *41*, 3739–3749.
[5] S. M. Zakeeruddin, M. Gratzel, *Adv. Funct. Mater.* **2009**, *19*, 2187–2202.
[6] P. Nockemann, B. Thijs, T. N. Parac-Vogt, K. Van Hecke, L. Van Meervelt, B. Tinant, I. Hartenbach, T. Schleid, V. T. Ngan, M. T. Nguyen, K. Binnemans, *Inorg. Chem.* **2008**, *47*, 9987–9999.
[7] H. Ohno, *Bull. Chem. Soc. Jpn.* **2006**, *79*, 1665–1680.
[8] Y. Yoshida, G. Saito, *Phys. Chem. Chem. Phys.* **2010**, *12*, 1675–1684.
[9] A. V. Mudring, S. F. Tang, *Eur. J. Inorg. Chem.* **2010**, 2569–2581.
[10] J. M. Lu, F. Yan, J. Texter, *Prog. Polym. Sci.* **2009**, *34*, 431–448.
[11] M. Armand, F. Endres, D. R. MacFarlane, H. Ohno, B. Scrosati, *Nat. Mater.* **2009**, *8*, 621–629.
[12] T. P. Lodge, *Science* **2008**, *321*, 50–51.
[13] A. Vioux, J. Le Bideau, L. Viau, *Chem. Soc. Rev.* **2011**, *40*, 907–925.
[14] E. Delahaye, Z. L. Xie, A. Schaefer, L. Douce, G. Rogez, P. Rabu, C. Gunter, J. S. Gutmann, A. Taubert, *Dalton Trans.* **2011**, *40*, 9977–9988.
[15] A. Neouze, J. Le Bideau, P. Gaveau, S. Bellayer, A. Vioux, *Chem. Mater.* **2006**, *18*, 3931–3936.
[16] A. Vioux, L. Viau, S. Volland, J. Le Bideau, *C. R. Chim.* **2010**, *13*, 242–255.
[17] F. Gayet, L. Viau, F. Leroux, F. Mabille, S. Monge, J. J. Robin, A. Vioux, *Chem. Mater.* **2009**, *21*, 5575–5577.
[18] R. Göbel, A. Friedrich, A. Taubert, *Dalton Trans.* **2010**, *39*, 603–611.
[19] M. A. Susan, T. Kaneko, A. Noda, M. Watanabe, *J. Am. Chem. Soc.* **2005**, *127*, 4976–4983.
[20] B. Singh, S. S. Sekhon, *J. Phys. Chem. B* **2005**, *109*, 16539–16543.
[21] S. Volland, M. Gruit, T. Regnier, L. Viau, O. Lavastre, A. Vioux, *New J. Chem.* **2009**, *33*, 2015–2021.
[22] Y. Xie, K. L. Ding, Z. M. Liu, J. J. Li, G. M. An, R. T. Tao, Z. Y. Sun, Z. Z. Yang, *Chem. Eur. J.* **2010**, *16*, 6687–6692.
[23] Z. L. Xie, H. B. Xu, A. Gessner, M. U. Kumke, M. Priebe, K. M. Fromm, A. Taubert, *J. Mater. Chem.* **2012**, *22*, 8110–8116.
[24] K. Lunstroot, K. Driesen, P. Nockemann, C. Gorller-Walrand, K. Binnemans, S. Bellayer, J. Le Bideau, A. Vioux, *Chem. Mater.* **2006**, *18*, 5711–5715.
[25] Z. L. Xie, A. Jelicic, F. P. Wang, P. Rabu, A. Friedrich, S. Beuermann, A. Taubert, *J. Mater. Chem.* **2010**, *20*, 9543–9549.
[26] J. Gao, J. G. Liu, W. M. Liu, B. Li, Y. C. Xin, Y. Yin, Jungu, Z. G. Zou, *Int. J. Electrochem. Sci.* **2011**, *6*, 6115–6122.
[27] J. Gao, J. G. Liu, W. M. Liu, J. L. Ye, Y. Zhou, J. Gu, T. Yu, Z. G. Zou, *Chin. J. Inorg. Chem.* **2009**, *25*, 2016–2020.
[28] J. S. Lee, T. Nohira, R. Hagiwara, *J. Power Sources* **2007**, *171*, 535–539.
[29] A. C. Marr, P. C. Marr, *Dalton Trans.* **2011**, *40*, 20–26.
[30] E. Delahaye, R. Göbel, R. Lobbicke, R. Guillot, C. Sieber, A. Taubert, *J. Mater. Chem.* **2012**, *22*, 17140–17146.
[31] F. Benito-Lopez, R. Byrne, A. M. Raduta, N. E. Vrana, G. McGuinness, D. Diamond, *Lab Chip* **2010**, *10*, 195–201.
[32] F. Benito-Lopez, S. Coyle, R. Byrne, V. F. Curto, D. Diamond, *IEEE Sens.* **2010**, 160–163.
[33] J. Lee, M. J. Panzer, Y. Y. He, T. P. Lodge, C. D. Frisbie, *J. Am. Chem. Soc.* **2007**, *129*, 4532–4533.
[34] Y. Y. He, P. G. Boswell, P. Buhlmann, T. P. Lodge, *J. Phys. Chem. B* **2007**, *111*, 4645–4652.
[35] Z. H. Li, J. Jiang, G. T. Lei, D. S. Gao, *Polym. Adv. Technol.* **2006**, *17*, 604–607.
[36] S. Coleman, R. Byrne, N. Alhashimy, K. J. Fraser, D. R. MacFarlane, D. Diamond, *Phys. Chem. Chem. Phys.* **2010**, *12*, 7009–7017.
[37] S. Hayashi, H. O. Hamaguchi, *Chem. Lett.* **2004**, *33*, 1590–1591.
[38] H. Cölfen, M. Antonietti, *Angew. Chem., Int. Ed.* **2005**, *44*, 5576.
[39] J. Jiang, D. S. Gao, Z. H. Li, G. Y. Su, *React. Funct. Polym.* **2006**, *66*, 1141–1148.
[40] V. V. Singh, A. K. Nigam, A. Batra, M. Boopathi, B. Singh, R. Vijayaraghavan, *Int. J. Electrochem.* **2012**, *2012*, 1–19.
[41] G. T. Kim, S. S. Jeong, M. Z. Xue, A. Balducci, M. Winter, S. Passerini, F. Alessandrini, G. B. Appetecchi, *J. Power Sources* **2012**, *199*, 239–246.
[42] Q. H. Zhang, S. G. Zhang, S. M. Liu, X. Y. Ma, L. J. Lu, Y. Q. Deng, *Analyst* **2011**, *136*, 1302–1304.